The Effects of Gusts on the Fluctuating Airloads of Airfoils in Transonic Flow

W. J. McCroskey*
NASA Ames Research Center, Moffett Field, California

Unsteady interactions of distributed and sharp-edged gusts with a stationary airfoil have been analyzed in two-dimensional transonic flow. A simple method of introducing such disturbances has been numerically implemented within the framework of unsteady transonic small-disturbance theory. Representative solutions for various airfoils subjected to chordwise and transverse gusts show that the strength and unsteady motion of the shock wave on the airfoil significantly affect the flowfield development and, consequently, the dynamic airloads. Also, a study was made of the reductions in the unsteady airloads that can be achieved by the proper active control motion of a trailing-edge flap, and a simple gust-alleviation strategy was developed. However, the chordwise pressure distributions associated with gusts are very different from those produced by trailing-edge flap oscillations. Consequently, this simple device cannot eliminate both the fluctuating lift and the unsteady pitching moments simultaneously.

I. Introduction

THE unsteady interaction of gusts and similar vortical disturbances with lifting surfaces often plays a significant role in the aerodynamics, dynamic loading, aeroelasticity, and acoustics of modern aircraft, missiles, helicopter rotors, and turbomachines. The interaction phenomena can be especially acute in the transonic flow regime, where shock wave positions and strengths are sensitive to small changes in the flow parameters and the resultant airloads may deviate significantly from the predictions of linear theory.

A previous paper[1] described the adaptation of an efficient two-dimensional transonic flow computer code to the interactions of strong *concentrated* vortices with airfoils, simulating the rotor blade/vortex interaction problem of helicopter aerodynamics. The application of the basic method to distributed disturbances, in the form of transverse gusts, was also discussed briefly. This paper concentrates on several aspects of the gust problem that have not been treated previously for transonic flow conditions, such as the onset of significant nonlinear effects, the differences between chordwise and transverse gusts, the differences between the gust-induced airloads on supercritical and conventional airfoils, and active control strategies for gust alleviation.

II. Formulation and Numerical Method

The problem is formulated within the framework of the transonic small-disturbance approximation for a thin airfoil in an inviscid, isentropic fluid, with small vortical disturbances superimposed on an otherwise uniform, nearly sonic freestream. These prescribed disturbances are assumed to convect with the mean freestream velocity U_∞ and to remain unaltered by the interaction with the airfoil. According to Goldstein and Atassi,[2] this latter assumption may not be justified in some cases, but it permits nonlinear transonic effects to be examined by a straightforward application of existing finite difference methods for cases that would presently be untractable otherwise.

The combination of unsteady flow and rotational disturbances in the freestream requires some special attention, if potential flow concepts and numerical algorithms are to be retained. However, the prescribed disturbance or perturbation methods of Refs. 1, 3, and 4 allow this to be done, as outlined below. Under the aforementioned assumptions, the governing equations are

continuity:

$$\frac{D\rho}{Dt}+\rho\nabla\cdot q=0 \tag{1}$$

momentum:

$$\frac{Dq}{Dt}+\frac{\nabla p}{\rho}=0 \tag{2}$$

and the relevant isentropic relations are

$$p/\rho^\gamma=\text{const} \tag{3a}$$

$$P=\int\frac{dp}{\rho}=\int a^2\frac{d\rho}{\rho}=\frac{a^2-a_0^2}{\gamma-1} \tag{3b}$$

Various Bernoulli equations are commonly derived as combinations of Eqs. (2) and (3), e.g., see Ref. 5, under the assumption that the flow is either irrotational or steady, or both. Here, we multiply Eq. (2) by an incremental position vector dr and integrate over a suitable path from an upstream reference point to obtain

$$\int\left(\frac{\partial q}{\partial t}-q\times\nabla\times q\right)\cdot dr+\frac{\nabla q^2}{2}+p=f(t) \tag{4}$$

Next we define a quantity Q, which plays a role analogous to a scalar potential for irrotational flow, but which is more

Presented as Paper 84-1580 at the AIAA 17th Fluid Dynamics, Plasma Dynamics, and Lasers Conference, Snowmass, Colo., June 25-27, 1984; received Aug. 18, 1984, revision received Dec. 17, 1984.

*Senior Staff Scientist, U.S. Army Aeromechanics Laboratory (AVSCOM) and NASA Astronautics Directorate. Associate Fellow AIAA.

general here, namely,

$$Q=\int\left(\frac{\partial q}{\partial t}-q\times\nabla\times q\right)\cdot dr-f(t) \tag{5}$$

With this definition, Eqs. 1 and 4 can be combined in the usual ways that are employed for steady rotational or unsteady irrotational flow, giving

$$\frac{\partial Q}{\partial t}+2q\cdot\frac{\partial q}{\partial t}+\tfrac{1}{2}q\cdot\nabla q^2+a^2\nabla\cdot q=0 \tag{6a}$$

or in two dimensions,

$$\frac{\partial Q}{\partial t}+2u\frac{\partial u}{\partial t}+2v\frac{\partial v}{\partial t}+(a^2-u^2)\frac{\partial u}{\partial x}$$

$$-uv\left(\frac{\partial u}{\partial y}+\frac{\partial v}{\partial x}\right)+(a^2-v^2)\frac{\partial v}{\partial y}=0 \tag{6b}$$

Finally, for small disturbances, $v\ll u$,

$$\frac{\partial Q}{\partial t}+2u\frac{\partial u}{\partial t}+(a^2-u^2)\frac{\partial u}{\partial x}+a^2\frac{\partial v}{\partial y}=0 \tag{7}$$

Up to this point, we have skirted the issue of what Q really represents and how it could be evaluated. Now we decompose the total velocity field into the following components: 1) a uniform freestream U_∞, 2) a prescribed far-field gust field q_G, and 3) an irrotational perturbation velocity field $\nabla\varphi$ due to the airfoil in the presence of the gust. That is,

$$q=U_\infty+q_G+\nabla\varphi \tag{8}$$

Then

$$Q=\frac{\partial\varphi}{\partial t}+\int\left(\frac{\partial q_G}{\partial t}-q\times\nabla\times q_G\right)\cdot dr \tag{9}$$

It should be emphasized that this decomposition of the velocity does not imply linearity. For the nonlinear cases considered in this paper, both the boundary conditions and the governing equation for the airfoil disturbance potential φ may be altered by the introduction of q_G; independent solutions are not superimposable.

The governing equation for φ is obtained by substituting first the quantity $q_o=U_\infty+q_G$ and then q given by Eq. (8) into Eq. (7). Next, the former resulting equation is substracted from the latter. Then the quantity

$$\int\left(\frac{\partial q_G}{\partial t}-q_o\times\nabla\times q_G\right)\cdot dr$$

which is common to both, drops out and

$$(\nabla\varphi\times\nabla\times q_G)\cdot dr=0$$

if dr is aligned with $\nabla\varphi$. Finally, the local speed of sound a is evaluated using the isentropic relations and the usual transonic small-disturbance scaling laws and approximations,[5,6] coupled with the observation that the prescribed disturbances considered herein produce only second-order variations in density, pressure, and temperature.[7,8] This gives the following modified form of the unsteady transonic small-disturbance equation (in strong conservation form):

$$M_\infty^2\varphi_{tt}+2M_\infty^2\varphi_{xt}=\frac{\partial}{\partial x}[(\beta^2+C_2\varphi_x)(\varphi_x+u_G)-\beta^2u_G]+\varphi_{yy} \tag{10}$$

where $\beta^2=1-M_\infty^2$ and $C_2=-\tfrac{1}{2}(\gamma+1)M_\infty^2$. Linear theory is recovered by setting $C_2=0$.

Similarly, the boundary condition on the airfoil is obtained by substituting Eq. (8) into the small-disturbance approximation to flow tangency, giving

$$\left(\frac{\partial\varphi}{\partial y}\right)_b=\left(\frac{\partial}{\partial t}+U_\infty\frac{\partial}{\partial x}\right)Y_{\text{body}}-v_G \tag{11}$$

As noted above, the small vortical disturbances produce no pressure fluctuations to first order in the freestream.[7,8] Therefore, consistent with the aforementioned assumption that the gust remains undistorted as it passes by the airfoil, we retain the small-disturbance pressure coefficient in its usual form,

$$C_p=-2(\varphi_t+\varphi_x) \tag{12}$$

Equation (10) has been solved using the numerical algorithm of the well-exercised transonic code LTRAN2[6] with the high-frequency terms included.[1] This latter improvement extends the range of validity of the original code and allows more accurate indicial-response calculations to be made. As discussed in Ref. 1 and in Sec. III, the revised code was checked out by comparing with linear theory for pitching oscillations of a thin airfoil and for the response of an airfoil to a sinusoidal transverse gust.

Finally, brief mention should be made of the related decomposition of the velocity field used by Goldstein,[7] Kerschen and Myers,[9] and others following Goldstein's lead. These investigators have dealt with the fully linearized form of the small-disturbance equations to order $\epsilon\alpha$, where ϵ is a small parameter denoting the magnitude of the gust and α a measure of the thickness or mean incidence of the airfoil. In the present notation, their decomposition would be

$$q=U+q_{G\infty}+\Delta q_G+\nabla\varphi' \tag{13}$$

where U is the steady solution of the mean flow past the airfoil; $q_{G\infty}$ the undistorted, prescribed gust field as before; $(q_{G\infty}+\Delta q_G)$ the distorted gust field due to the mean flow U, i.e., $u^{(I)}$ in Goldstein's notation; and φ' the first-order irrotational perturbation caused by the gust. Including the effect of the distortion of the gust as it convects past the airfoil goes beyond the present investigation in that sense, but the nonlinear interactions associated with transonic flows have not been considered. Combining the two analyses would be more complete and exact, but much more complicated, since the function Q would have to be dealt with explicitly and on a case-by-case basis.

III. Periodic Transverse and Horizontal Gusts

Numerical calculations have been performed for a number of transonic flows with sinusoidal gust fields, corresponding to examples that have already appeared in the literature for incompressible or subsonic flows. These results illustrate the special phenomena that arise in periodic flowfields with moving shock waves.

Symmetrical Airfoil, Sinusoidal Transverse Gust

The first case to be considered is the transonic counterpart of the well-known[10,11] sinusoidal traveling-wave gust with a transverse velocity

$$v_G=A_1\sin(\omega t-\omega\tilde{x}) \tag{14}$$

where $\tilde{x}/c=2x-1$ is measured from the midchord of the airfoil and c is the chord. This case is particularly straightfor-

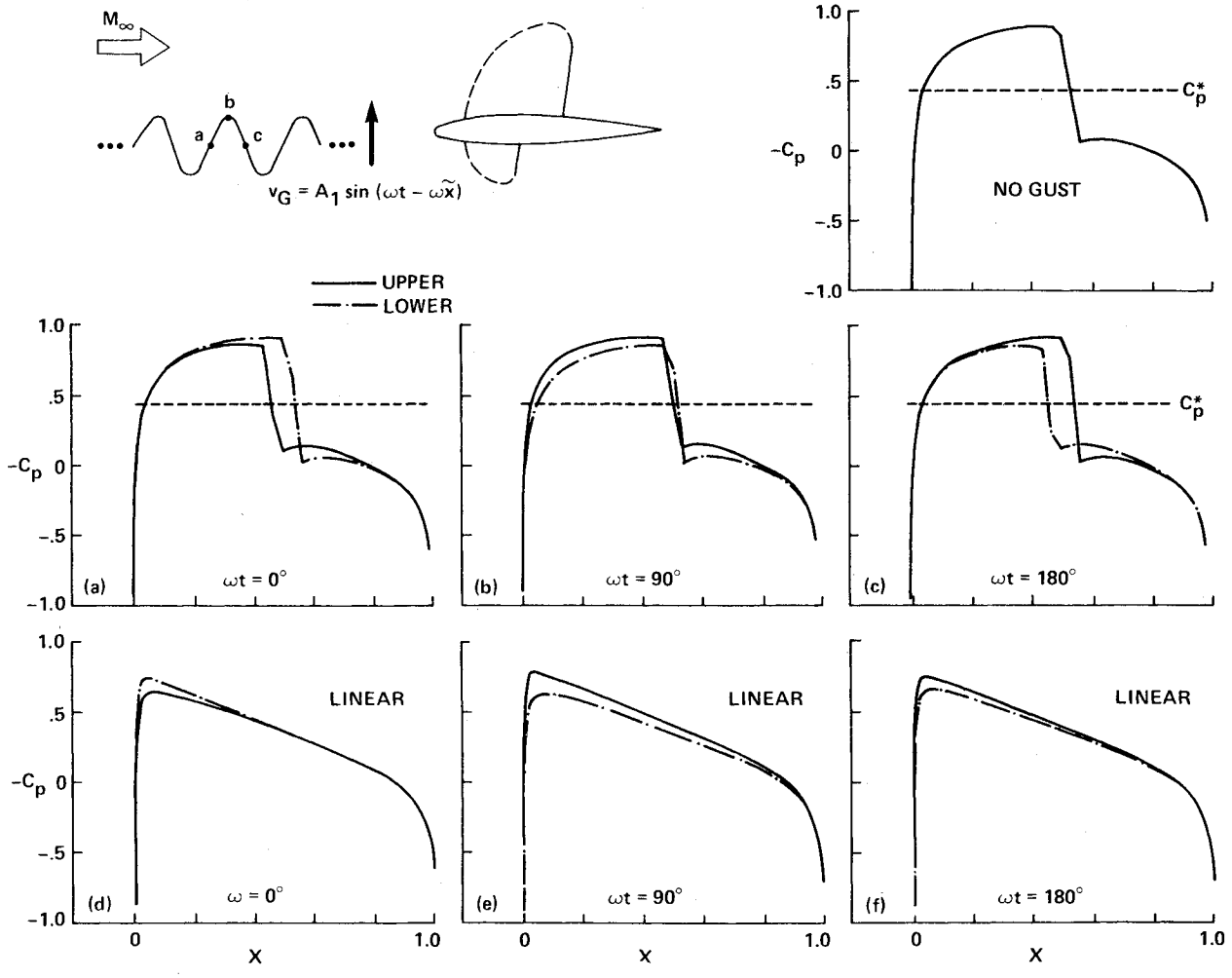

Fig. 1 Instantaneous pressure distribution due to a sinusoidal transverse gust: NACA 0012 airfoil, $M_\infty = 0.80$, $\alpha = 0$, $A_1 = 0.017$, $K_G = \omega c/U_\infty = 0.50$.

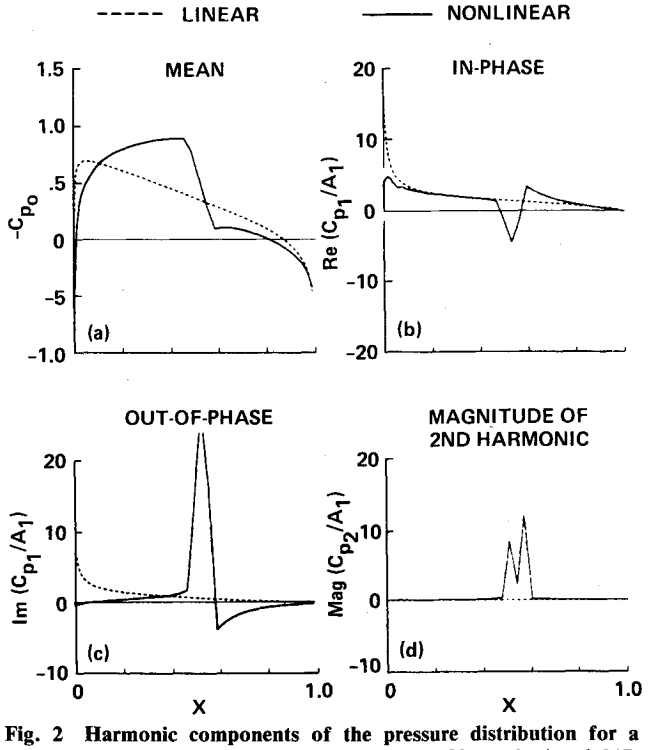

Fig. 2 Harmonic components of the pressure distribution for a sinusoidal transverse gust: NACA 0012, $M_\infty = 0.80$, $\alpha = 0$, $A_1 = 0.017$, $K_G = 0.50$.

ward within the framework of the transonic small-disturbance approximation, since the gust velocity does not enter explicitly in the governing equation. The effect of the gust is felt through the boundary condition on the airfoil as an effective time- and space-dependent angle of attack [Eq. (11)].

A sketch of this problem and typical results for this type of gust are shown in Fig. 1, computed for both the nonlinear and linear ($C_2 = 0$) mode of Eq. (10) at various "phases" during the passage of the gust. Figure 2 shows the harmonic components of the upper-surface pressure distribution, referenced to the phase and amplitude of the prescribed gust; the lower-surface pressures (not shown) are equal in magnitude and opposite in sign for this case of a symmetrical airfoil at zero incidence. The nondimensional frequency parameter, $K_G = \omega c/U_\infty$, is inversely proportional to the wavelength λ of the gust; $\lambda = 2\pi U_\infty/\omega = 4\pi c$ in this particular case. The amplitude of the gust corresponds to an effective angle of attack of 1 deg in this and in all of the following examples, unless otherwise noted.

The main distinction of the nonlinear solution from linear theory is the presence of a shock wave and its unsteady motion as the gust passes by. This motion is the reason for the large spikes in the harmonic components of the pressure coefficient (Fig. 2), sometimes called a "shock doublet" in the literature.[12,13] The second- and higher-harmonic content is essentially zero except for the section of the airfoil over which the shock wave moves.

Figure 3 shows the amplitude and phase of the fluctuating lift produced by gusts of different frequencies, or wave lengths, for the NACA 0012 airfoil at zero mean incidence.

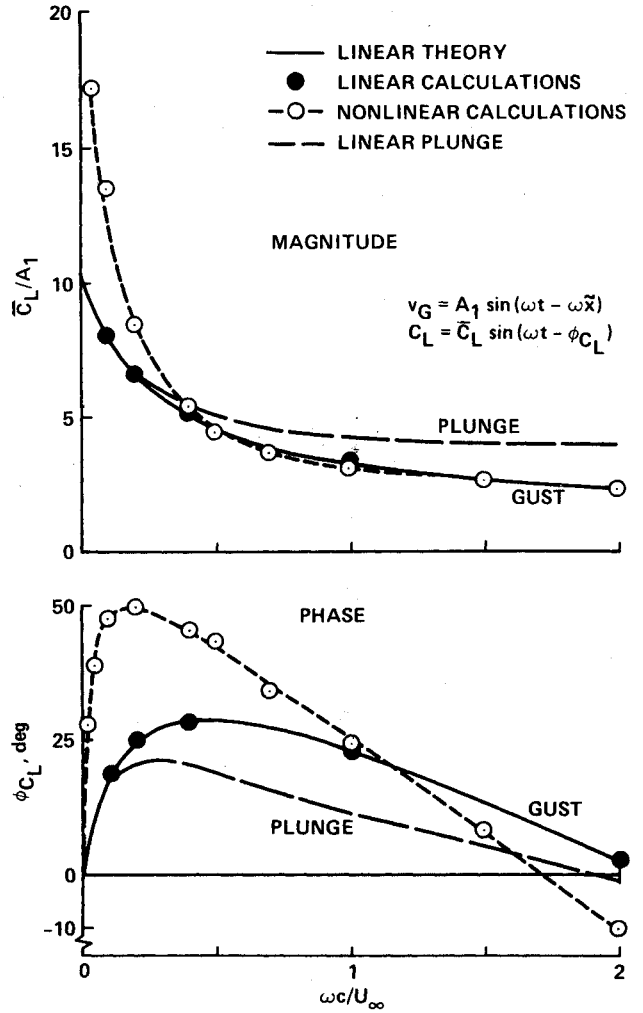

Fig. 3 Lift response to a sinusoidal transverse gust: NACA 0012, $M_\infty = 0.80$, $\alpha = 0$, $A_1 = 0.017$, (1 deg).

Also shown for reference are the results of the present linear calculations and those of Graham[11] and linear theory for sinusoidal plunging oscillations of an airfoil in a uniform stream. The magnitude of the nonlinear unsteady gust response is much higher than the linear value at low reduced frequencies, whereas the two types of linear problems, gust and plunge, are almost identical for $K < 0.4$. However, the two linear results diverge for $K > 0.4$; on the other hand, the nonlinear and linear gust solutions essentially merge at the higher reduced frequencies.

The phases of the linear and nonlinear fluctuating lift relative to the gust velocity at midchord are seen to be significantly different over almost the whole frequency range. The pitching moment behavior, not shown, follows similar trends, except that the nonlinear magnitudes of C_M for the sinusoidal gust problem only merge into the linear values for $K > 1$.

Conventional vs Supercritical Airfoil Gust Response

Computed results for the Dornier CAST-7 supercritical airfoil[14] and the conventional NACA 0012 airfoil are compared in Fig. 4. The gust wavelength for these results is the same as in Figs. 1 and 2, but significant amounts of lift are developed in this example and the nonlinear effects are stronger on the upper surface than before. It is interesting to note that upper-surface shock wave is much stronger on the NACA 0012 than on the CAST-7 airfoil, with correspondingly larger magnitudes of the shock-doublet spike. However, the shock wave

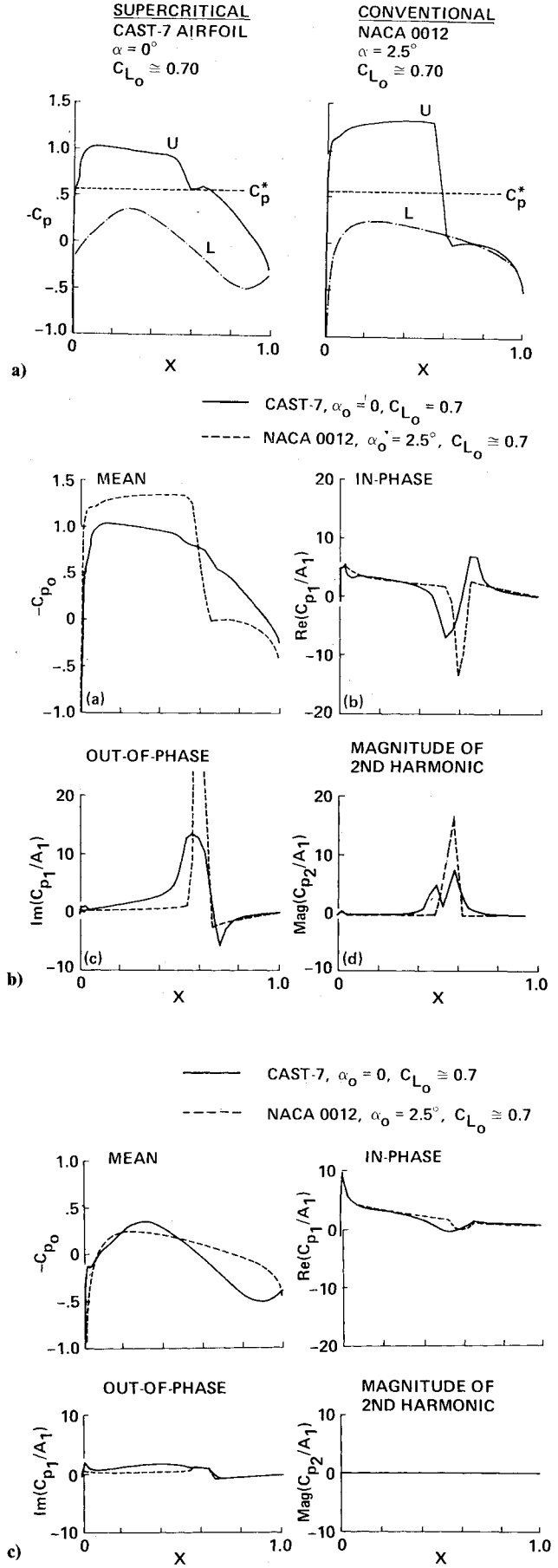

Fig. 4 Comparison of gust response on highly-loaded airfoils at $M = 0.76$: $A_1 = 0.017$, $K_G = 0.50$: a) steady solutions at the mean angle of attack; b) upper-surface harmonic pressure distributions; c) lower-surface harmonic pressure distributions.

motion is much greater on the CAST-7 airfoil, to the extent that the mean C_p distribution in Fig. 4b is significantly different from the C_p distribution without the gust (Fig. 4a).

The lower surfaces of both airfoils remain subcritical throughout most of the cycle of the gust interaction. Consequently, both curves of mean C_p in Fig. 4c are approximately equivalent to the respective lower-surface steady values in Fig. 4a, there is negligible higher-harmonic content, and the fluctuating pressures more nearly resemble the linear solutions shown in Fig. 2.

It is also interesting to note that the differences in the results between the two airfoils are significantly less than those between the NACA 0012 at zero lift (Fig. 2) and high lift (Fig. 4). Thus, the extent of supersonic flow and the strength of the shock wave appear to be more important than the actual details of the airfoil geometry. It is clear that linear theory is inadequate in any of the cases with significant shock-wave motion.

Streamwise vs Transverse Gusts

The second type of gust to be considered is a periodic streamwise velocity perturbation,

$$u_G = A_I \sin(\omega t - \omega \tilde{x}) \tag{15}$$

where, as before, $\tilde{x}/c = 2x - 1$ is measured from the midchord of the airfoil. In the incompressible linear case, Horlock,[15] Morfey,[16] and Goldstein and Atassi[2] have identified three primary effects of this type of gust on the unsteady airloads. First, the surface speed distribution is altered symmetrically on the upper and lower surfaces of the airfoil, producing no net lift to first order with respect to the gust amplitude. Second, the vorticity distribution on a lifting airfoil couples with the fluctuating streamwise velocity to produce fluctuating lift and pitching moment that are proportional to the mean (time-average) lift. This falls into the category of the second-order $\mathcal{O}(\epsilon\alpha)$ effects mentioned at the end of Sec. II; and Horlock[15] has derived an analytical solution to account for it. Third, the distortion of the gust by the mean flow field of the lifting airfoil is also a second-order effect $\mathcal{O}(\epsilon\alpha)$, which Goldstein and Atassi[2] claim to be as important as the basic phenomenon treated by Horlock.

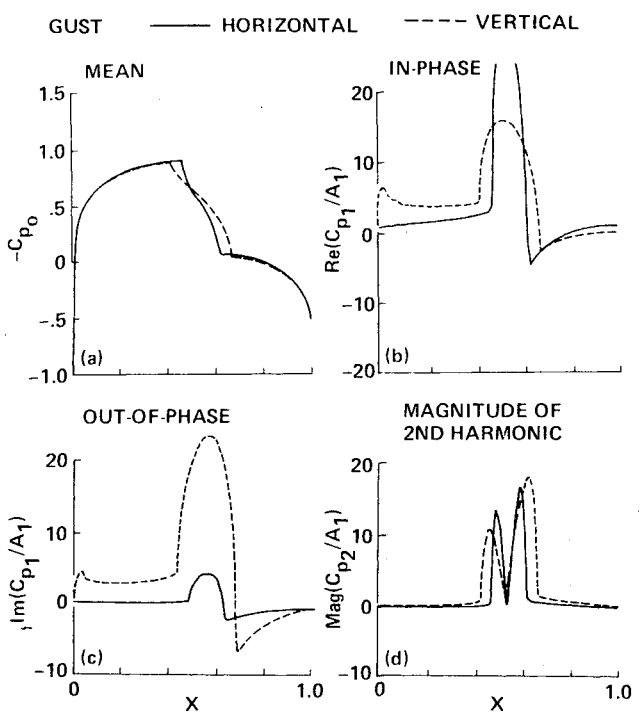

Fig. 5 Comparison of horizontal and vertical gust response: NACA 0012, $M_\infty = 0.80$, $\alpha = 0$, $A_I = 0.017$, $K_G = 0.10$.

The first and second effects outlined in the previous paragraph are automatically captured by the present numerical method in either subsonic or transonic flow. Unfortunately, the gust-distortion effect is much more difficult to analyze and its importance in the transonic regime remains unknown. It also violates one of the key assumptions of this paper, and thus lies outside the present scope. Consequently, we shall consider only the first of the three effects outlined above; namely, the effects of a purely chordwise gust on the symmetrical mean pressure distribution. This becomes a first-order effect as $M_\infty \to 1$, according to our transonic small-disturbance formulation.

Figures 5 and 6 show a comparison of the harmonic pressure distributions due to chordwise and transverse gusts. These results are for the same Mach number and airfoil that

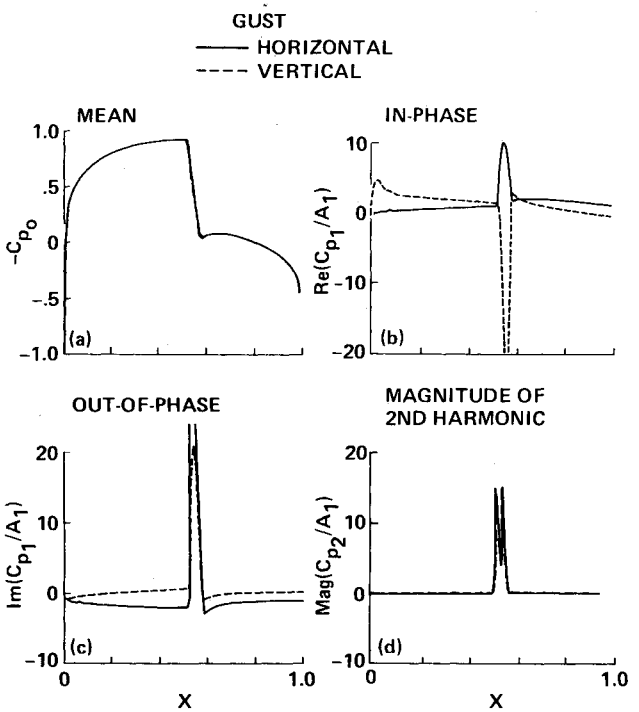

Fig. 6 Comparison of horizontal and vertical gust response: NACA 0012, $M_\infty = 0.80$, $\alpha = 0$, $A_I = 0.017$, $K_G = 1.0$.

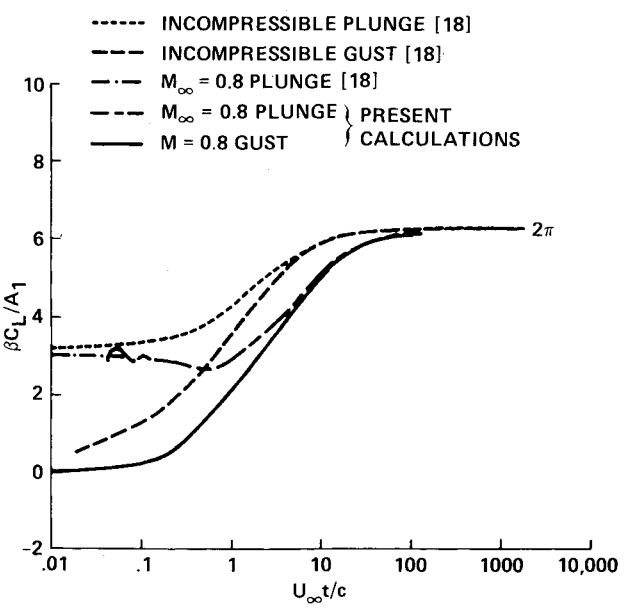

Fig. 7 Linear indicial lift response.

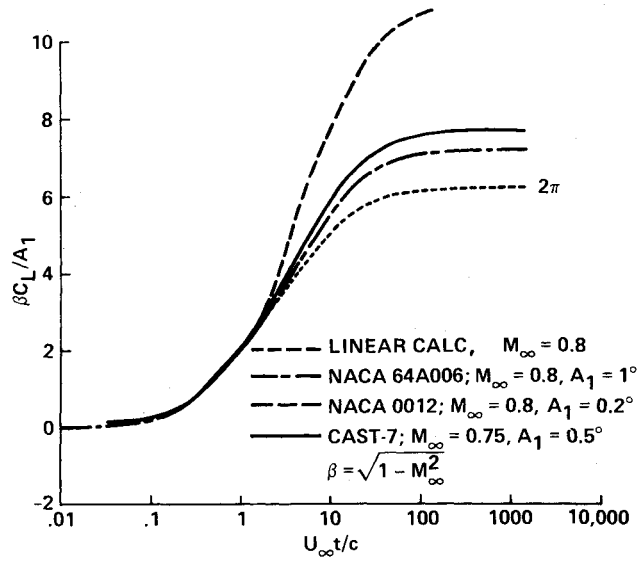

Fig. 8 Nonlinear indicial lift response.

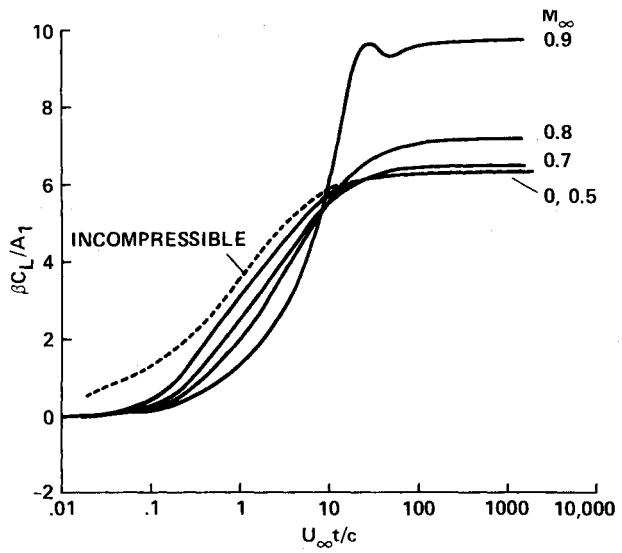

Fig. 9 Nonlinear indicial lift response for a sharp-edged gust: NACA 64A006 airfoil, $A_1 = 0.017$ (1 deg).

were considered in Figs. 1-3, but for higher and lower reduced frequencies. In both figures and for both types of gust, large shock-doublet spikes are evident, again due to the oscillatory motion of the shock waves. However, the solutions at each frequency are significantly different, just as the solutions for a given type of gust differ greatly at the two different frequencies because of the differing shock wave motions.

In a qualitative sense, the two types of gusts produce pressure fluctuations of comparable overall magnitude in the vicinity of the moving shock waves. This transonic behavior contrasts importantly with the concentrated-vortex cases considered in Ref. 1, where the effect of the u component of the vortex was shown to be much less than the effect of the v component.

IV. Sharp-Edged Gusts—The Indicial Problem

Ballhaus and Goorjian[17] showed how transonic indicial solutions can be used to advantage in oscillating airfoil problems with small-amplitude motions. The validity of this approach is generally limited to cases in which the shock wave motion is negligible and the unsteady fluctuations are essentially linear perturbations about a nonlinear steady or mean flow. Although the preceding examples tended not to satisfy this condition, situations with smaller-amplitude gusts or weaker shock waves would be amenable to the indicial method.

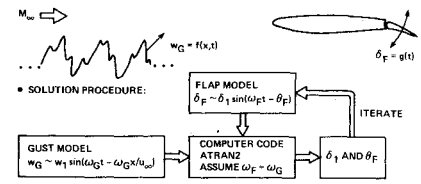

Fig. 10 Reduction of gust-induced airloads by a trailing-edge flap.

Figure 7 shows a comparison of the linear response of a thin airfoil at $M_\infty = 0$ and 0.80 to two types of indicial inputs, namely,

plunge:

$$\alpha = \begin{cases} 0 \text{ for } t<0 \\ A_1 \text{ for } t>0 \end{cases} \tag{16}$$

gust:

$$v_G = \begin{cases} 0 \text{ for } U_\infty \epsilon < x \\ A_1 \text{ for } U_\infty t > x \end{cases} \tag{17}$$

Both gust responses rise monotonically from zero at $t=0$ to the value $C_L = 2\pi A_1/(1-M_\infty^2)^{1/2}$ as $t \to \infty$, whereas the plunge responses[18] start at $C_L = \pi A_1$ for $M_\infty = 0$ and at $4A_1/M_\infty$ for $M_\infty > 0$. In either case, the approach to the steady-state value is progressively slower as M_∞ increases.

A comparison of some mildly nonlinear indicial gust responses for several different airfoils is shown in Fig. 8. The Mach number is 0.80 for these results, with the exception of the CAST-7 airfoil, for which meaningful steady-state solutions could not be obtained at this Mach number.

The solution for the NACA 64A006 at $M_\infty = 0.80$ is only slightly supercritical as the asymptotic steady state corresponding to $\alpha = 1$ deg is approached and, consequently, the lift response is not much different from the linear solution. Nonlinear effects are slightly more important for the CAST-7 airfoil under these particular conditions and much more important for the NACA 0012, even though the amplitude of the gust is only 0.2 deg.

Fig. 9 shows the effect of Mach number on the gust response of the NACA 64A006 airfoil. The overshoot in lift at $M_\infty = 0.9$ is due to a complex, nonlinear motion of the shock wave on the *lower* surface. The upper-surface shock wave moves monotonically rearward from its initial position of $X \approx 0.85$ and stabilizes at the trailing edge at $U_\infty t/c \approx 25$.

In both Figs. 8 and 9, the most significant transonic effects tend to occur for $U_\infty t/c > 10$, when the changes in the flowfield are occurring less rapidly. This behavior corresponds closely to the effects of reduced frequency that were illustrated previously in Figs. 3, 5, and 6, wherein the low-frequency, or long-wavelength, sinusoidal gusts perturbed the mean flow more significantly, and with greater higher-harmonic content, than did the high-frequency gusts.

V. Strategies for Gust Alleviation

A number of calculations were performed to examine the possibility of cancelling gust-induced unsteady airloads by the appropriate motion of a simple trailing-edge flap, using the combined capability of the original LTRAN2 code and the present modifications for calculating the gust response. The basic strategy is outlined in Fig. 10. Starting with a specified gust wave form, we perform the first iteration as if the pro-

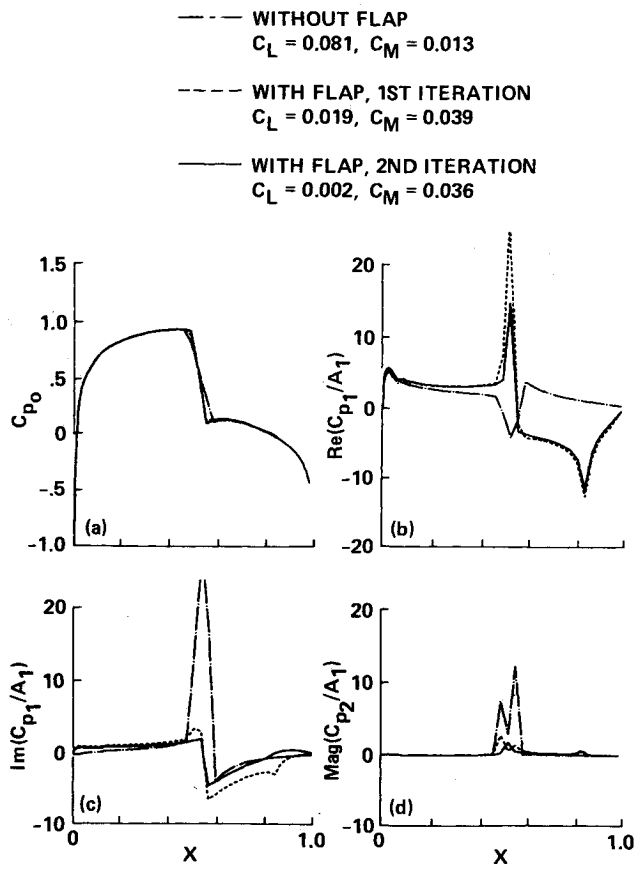

Fig. 11 Gust alleviation by a trailing-edge flap: NACA 0012 airfoil, $M_\infty = 0.80$, $\alpha = 0$, $A_1 = 0.017$, $K_G = 0.50$.

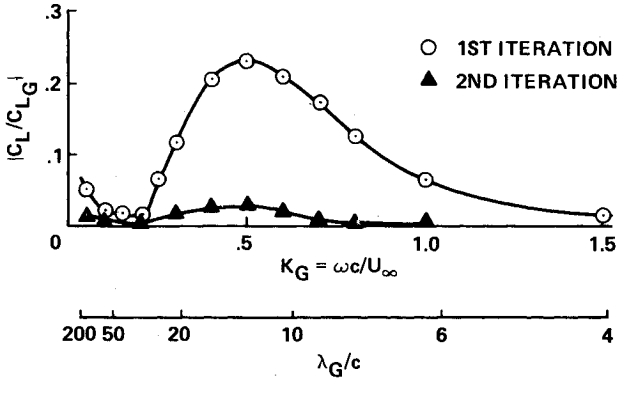

Fig. 12 Reduction in the gust-induced unsteady lift by a trailing-edge flap: NACA 0012, $M_\infty = 0.80$, $\alpha = 0$, $A_1 = 0.017$.

blem were linear and superposition were valid; that is, the flap is deflected so as to produce a lift that is equal and opposite to that caused by the gust. For the sinusoidal gusts considered above, this requires

$$\delta_F = -\delta_1 \sin(\omega t - \Theta_1) \tag{18}$$

where $\delta_1 = G/F$; $\Theta_1 = \theta_G - \theta_F$; G and θ_G are the magnitude and phase of the unsteady lift due to the gust, but without flap deflections; and F and θ_F are the magnitude and phase of the unsteady lift due to a flap deflection of unit magnitude and reduced frequency K_G in a uniform freestream.

As we shall see below, this first cycle of calculations reduces the gust response substantially. In some cases, however, nonlinear effects are so strong that a second iteration may be desired. This can be accomplished as follows:

$$\delta_F = -\delta_1 \sin(\omega t + \Theta_1) - \delta_2 \sin(\omega t + \Theta_2) + \cdots \tag{19}$$

where $\delta_i = G_i/F$; $\Theta_i = \theta_{Gi} - \theta_F$; and $i = 1,2,\cdots$; and Eq. (18) is used to specify the amplitude δ_1 and phase Θ_1. Then the resulting response, G_2 and θ_{G_2}, are used to determine $\delta_2 = G_2/F$ and $\Theta_2 = \theta_{G_2} - \theta_F$, etc.

Figure 11 shows the resultant pressure distributions for the example given previously in Figs. 1 and 2 after the first and second iterations of the gust iteration strategy. In this case, the magnitude of the unsteady lift coefficient is reduced by about a factor of four, from 0.081 to 0.019, after one iteration, although the pitching moment actually increases. The second iteration reduces C_L to 0.0022 and the higher-harmonic content becomes negligible.

The reduction in the magnitude of the unsteady lift by this strategy is shown in Fig. 12 for a range of gust frequencies or wavelengths. In this figure, C_{L_G} is the basic gust response *without* the flap, G_1, and C_L is the net response *with* the flap deflected according to Eq. (19). The results show that the lift response is reduced by an order of magnitude or more at low and high gust frequencies with only one iteration, but the mid-frequency range requires two iterations.

Figure 11 shows that, even though the lift was essentially cancelled, the unsteady pressure fluctuations remained large. Furthermore, this behavior was observed over the entire range of gust frequencies shown in Fig. 12. In fact, these fluctuating pressures produced significantly larger pitching moments for $K \gtrsim 0.1$ with flap oscillation than without. Conversely, attempts to reduce the pitching moment by the same strategy generally produced larger fluctuating lift. The basic difficulty is that the gust-induced loading tends to be centered close to the quarter chord, whereas trailing-edge flap deflections produce an aft loading. These differences are clearly evident in the figures and they tend to be even more acute in transonic flow than in purely subsonic flow. This phenomenon amounts to a fundamental difficulty for active control systems that rely solely on trailing-edge flaps, since it appears to be impossible to surpress both C_L and C_M with such a flap. Some of the advantages of combined leading- and trailing-edge flaps[19] or spoilers[20] over a single trailing-edge flap have been pointed out heretofore, but perhaps the present results and discussion will provide alternate and additional insights into the aerodynamic aspects of various active control systems.

VI. Summary and Conclusions

Transonic small-disturbance theory has been extended to include distributed vortical disturbances superimposed on a uniform freestream, under the assumption that the prescribed disturbance remains undistorted as it convects past a thin airfoil. A number of unsteady airfoil/gust interactions have been calculated within this framework, using a modified form of the well-established numerical code LTRAN2.[6] Sample results illustrate the essential effects of transverse and streamwise periodic gusts on the transonic flow around conventional and supercritical airfoils. Also, several examples of sharp-edged gusts have been studied, including the dependence of the indicial lift response upon Mach number, airfoil geometry, mean angle of attack, and amplitude of the gust. In all cases, the strength and unsteady motion of the shock wave were found to play major roles in the flowfield development and, consequently, in the airloads on the airfoil.

Combined gust response and oscillating control surfaces were also examined, with the aim of reducing the gust-induced airloads by activating a trailing-edge flap. A simple but effective strategy was developed for suppressing *either* the gust-induced lift *or* pitching moment by oscillating the flap with the proper phase and amplitude. However, the chordwise pressure distributions associated with gusts are very different from

those produced by trailing-edge flap oscillations. Consequently, this simple device cannot cancel both the fluctuating lift and pitching moments.

References

[1]McCroskey, W. J. and Goorjian, P. M., "Interactions of Airfoils with Gusts and Concentrated Vortices in Unsteady Transonic Flow," AIAA Paper 83-1691, July 1983.

[2]Goldstein, M. E. and Atassi, H., "A Complete Second-Order Theory for the Unsteady Flow About an Airfoil Due to a Periodic Gust," *Journal of Fluid Mechanics*, Vol. 74, P. 4, 1976, pp. 741-765.

[3]Steinhoff, J. and Suryanarayanan, K., "The Treatment of Vortex Sheets in Compressible Potential Flow," AIAA Paper 83-1881, July 1983.

[4]Buning, P. G. and Steger, J. L., "Solution of the Two-Dimensional Euler Equations with Generalized Coordinate Transformation Using Flux Vector Splitting," AIAA Paper 82-0971, June 1982.

[5]Liepmann, H. and Roshko, A., *Elements of Gasdynamics*, John Wiley & Sons, New York, 1957, pp. 180-200.

[6]Ballhaus, W. F. and Goorjian, P. M., "Implicit Finite-Difference Computations of Unsteady Transonic Flows about Airfoils," *AIAA Journal*, Vol. 15, Dec. 1977, pp. 1728-1735.

[7]Goldstein, M. E., "Unsteady Vortical and Entropic Distortions of Potential Flows Round Arbitrary Obstacles," *Journal of Fluid Mechanics*, Vol. 89, P. 3, 1978, pp. 433-468.

[8]Kovásznay, L. S. G. "Turbulence in Supersonic Flow," *Journal of the Aeronautical Sciences*, Vol. 20, Oct. 1953, pp. 657-674.

[9]Kerschen, E. J. and Myers, M. R. "Incidence Angle Effects on Convected Airfoil Noise," AIAA Paper 83-0765, May 1983.

[10]Sears, W. R., "Some Aspects of Non-Stationary Airfoil Theory and Its Practical Application," *Journal of the Aeronautical Sciences* Vol. 8, March 1941, pp. 104-108.

[11]Graham, J. M. R., "Similarity Rules for Thin Airfoils in Non-Stationary Subsonic Flows," *Journal of Fluid Mechanics*, Vol. 43, P. 4, 1970, pp. 753-766.

[12]Ashley, H., "Role of Shocks in the Sub-Transonic Flutter Phenomenon," *AIAA Journal*, Vol. 17, March 1980, pp. 187-197.

[13]McCroskey, W. J., "Unsteady Airfoils," *Annual Review of Fluid Mechanics*, Vol. 14, 1982, pp. 285-311.

[14]"Experimental Data Base for Computer Program Assessment," AGARD Advisory Rept. 138, 1979.

[15]Horlock, J. H., "Fluctuating Lift Forces on Aerofoils Moving through Tranverse and Chordwise Gusts," *Journal of Basic Engineering, Transactions of ASME*, Vol. 90, Ser. D, Dec. 1968, pp. 494-500.

[16]Morfey, C. L., "Lift Fluctuations Associated with Unsteady Chordwise Flow Past an Airfoil," *Journal of Basic Engineering, Transactions of ASME*, Vol. 92, Ser. D, Sept. 1970, pp. 663-664.

[17]Balllhaus, W. R. and Goorjian, P. M., "Computation of Unsteady Transonic Flows by the Indicial Method," *AIAA Journal*, Vol. 16, Feb. 1978, pp. 117-124.

[18]Lomax, H. "Indicial Aerodynamics," *AGARD Manual on Aeroelasticity*, Vol. II, Oct. 1968, Ch. 6; also NACA Rept. 1077, 1952.

[19]Nissim, E., "Comparative Study between Two Different Active Flutter Suppression Systems," *Journal of Aircraft*, Vol. 15, Dec. 1978, pp. 843-848.

[20]Mabey, D. G., "A Review of Some Recent Research on Time-Dependent Aerodynamics," *Aeronautical Journal*, Vol. 88, No. 872, Feb. 1984, pp. 23-37.